JOURNAL OF MATERIALS SCIENCE 28 (1993) 6360–6364

Microstructural evolution and threshold stress for superplastic flow in the Zn–Al eutectoid

S. TANDON, G. S. MURTY
Department of Metallurgical Engineering, Indian Institute of Technology, Kanpur 208 016, India

The microstructural evolution and the stress–strain rate behaviour of superplastic Zn–Al eutectoid alloy were investigated by prestraining specimens at two strain rates corresponding to Regions I and II. Even though the scale of microstructure was similar, the stress–strain rate curves of differently prestrained specimens were distinctly different in the lower strain-rate regime. While Region I of low rate sensitivity was more prominent when prestrained at a lower strain rate of Region I, it was less distinct because of prestrain in Region II. The threshold stress for superplastic flow, as assessed by an extrapolation procedure, varied with the nature of prestrain. The interphase boundaries were more rounded (higher mean curvature) on prestraining on Region II, compared to Region I. The correlation between the changes in the mean curvature of phase boundaries and the threshold stress arising from the nature of prestrain was consistent with the boundary-migration controlled sliding mechanism to interpret the threshold stress for superplastic flow.

1. Introduction

The flow stress (σ)–strain rate ($\dot{\varepsilon}$) relation and the influence of microstructure on it, in fine-grained materials are of interest in assessing superplastic flow mechanisms and exploring the possibility of superplastic forming. In general, the double logarithmic σ–$\dot{\varepsilon}$ plots of superplastic materials are sigmoidal in nature and are divided into Regions I, II and III [1]. The intermediate Region II of maximum rate sensitivity index, m, is the superplastic region. From observations on the transition from Region II to I in the Zn–Al eutectoid, various trends of either an increase or a decrease in m, or both, have been reported [2–4]. The Nabarro–Herring–Coble diffusional flow is likely to be responsible for an increase in m at low strain rates. Region I of low m has been explained in terms of either a threshold stress for superplastic flow [1, 5, 6] or an independent flow mechanism [3, 7, 8]. Some recent investigations [5, 6, 9–11] on rapidly solidified aluminium alloys and the Zn–Al eutectoid alloy, indicate that Region I of low m can be rationalized in terms of a temperature-and grain-size dependent threshold stress for superplastic flow. This interpretation of Region I in terms of a threshold stress was recently examined in terms of microstructural evolution effects arising from varying prestrain history [11, 12]. The manifestation of Region I in such experiments is observed to vary widely without any apparent change in the microstructures [11, 12]. The microstructural evolution effects on the σ–$\dot{\varepsilon}$ behaviour of the Zn–Al eutectoid alloy were explicitly explored in the present investigation in order to interpret them in terms of a threshold stress for superplastic flow.

2. Experimental procedure

A commercial Zn–Al eutectoid alloy with 23.55 wt % Al and 0.43 wt % Cu was used in this study. Sheet tensile specimens of 14 mm gauge length, 6 mm gauge width and 2 mm thickness were solution treated at 633 K for 18 h and quenched in water. The tensile tests were conducted in the as-quenched state and on samples of different grain sizes obtained by annealing at 523 K for varying times. Some of these specimens were prestrained at different temperatures and crosshead speeds. The true stress–true strain rate data were obtained by the strain-rate change test [13] making use of an Instron machine. The tensile tests were carried out at 448 and 473 K by employing an oil bath with a temperature control of $\pm 1^{\circ}$ C. Metallographic examination of shoulder and gauge sections of deformed tensile specimens was made by scanning electron microscopy in order to characterize their grain sizes. The grain size, d, reported here is 1.75 $\bar{l}$, where $\bar{l}$ is the mean linear intercept length measured from scanning electron micrographs.

3. Results

The microstructural evolution effects were studied with specimens in the grain size range of 1.4–3.5 μm. Typically, specimens were prestrained to a true strain of 0.4 at two initial strain rates, one of Region I and the other Region II. The stress–strain rate behaviour of specimens with and without prestrain was assessed by the strain-rate change test. The results presented in Figs 1–3 illustrate the differences in their stress–strain rate response and these are summarized below.

0022–2461 © *1993 Chapman & Hall*

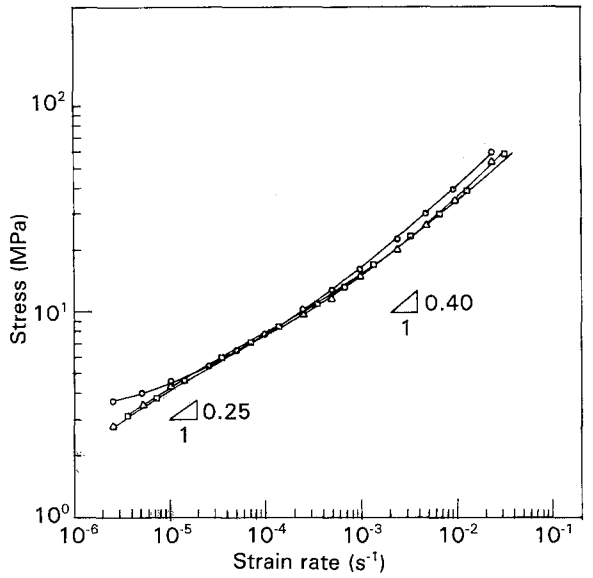

Figure 1 Stress–strain rate plots for specimens of finer grain size tested at 448 K. (□) No prestrain, $d = 1.7$ μm; (△) prestrained to $\varepsilon = 0.4$ at $\dot{\varepsilon} = 1.2 \times 10^{-2}\ s^{-1}$, $d = 1.5$ μm; (○) prestrained to $\varepsilon = 0.4$ at $\dot{\varepsilon} = 1.2 \times 10^{-4}\ s^{-1}$, $d = 1.9$ μm.

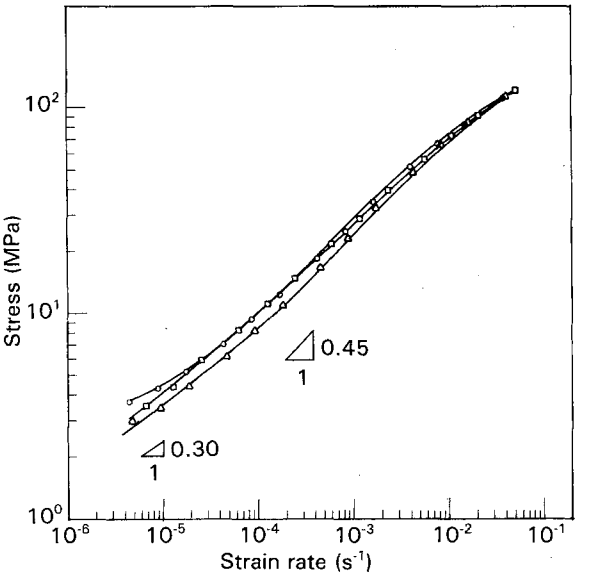

Figure 3 Stress–strain rate plots for coarser grained specimens tested at 473 K. (□) No prestrain, $d = 2.9$ μm; (△) prestrained to $\varepsilon = 0.4$ at $\dot{\varepsilon} = 6.0 \times 10^{-3}\ s^{-1}$, $d = 3.4$ μm; (○) prestrained to $\varepsilon = 0.4$ at $\dot{\varepsilon} = 6 \times 10^{-5}\ s^{-1}$, $d = 3.5$ μm.

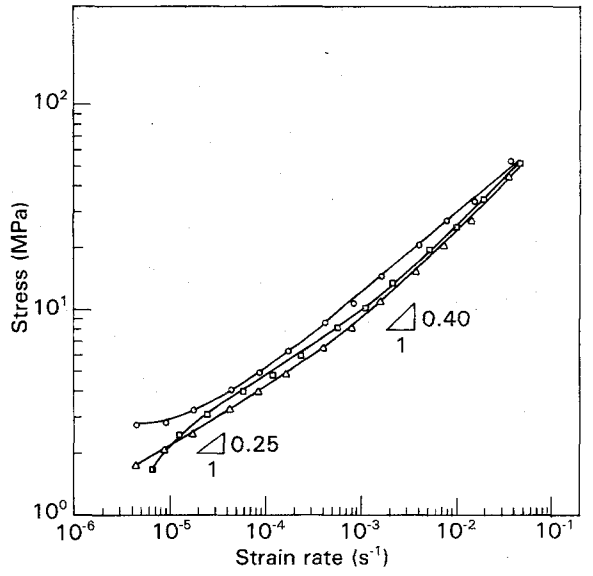

Figure 2 Stress–strain rate plots for specimens of finer grain size tested at 473 K. (□) No prestrain, $d = 1.4$ μm; (△) prestrained to $\varepsilon = 0.4$ at $\dot{\varepsilon} = 1.2 \times 10^{-2}\ s^{-1}$, $d = 1.4$ μm; (○) prestrained to $\varepsilon = 0.4$ at $\dot{\varepsilon} = 1.2 \times 10^{-4}\ s^{-1}$, $d = 1.5$ μm.

The maximum m value (0.4–0.45) of Region II is not affected by the nature of prestrain. While the transition from Region II to Region I of low m is evident in all tests at 448 and 473 K, the stress–strain rate curves differ significantly at low strain rates (around $10^{-5}\ s^{-1}$) depending on grain size, test temperature and prestrain history. Considering the first set of specimens without prestrain, a transition to a region of higher m (>0.5) is evident at lower strain rates and 473 K (Fig. 2) for the grain size 1.4 μm. On the other hand, specimens of coarser grain size (2.9 μm) do not exhibit such a transition at 473 K (Fig. 3). In the other category of varying prestrain history, there is a distinct difference in the stress–strain rate response at low strain rates depending on the strain rate of prestrain. On prestraining at a strain rate of Region I, the low m Region I is more prominent, whereas it is not so when prestrained at a higher strain rate of Region II. The grain-size data for specimens of varying prestrain history presented in Table I indicate minor changes in grain size because of the prestrains at lower (Region I) and higher (Region II) strain rates employed in this study. Various microstructures arising from differing prestrain history are illustrated in Figs 4 and 5 for coarser grained specimens. The microstructures of Fig. 5 correspond to those of Fig. 4b and c and these are presented at a higher magnification in order to distinguish the curvature of phase boundaries.

4. Discussion

4.1. Threshold stress evaluation

From the above results it is apparent that the stress–strain rate response of differently prestrained specimens is influenced by microstructural evolution other than variation in grain size. Hence the influence of prestrain history on the shape of the stress–strain rate curve cannot be rationalized in terms of grain-size variations arising from prestrain history. Other microstructural features such as the sizes of each phase, the inhomogeneity in the distribution of two phases and the non-equiaxed grains are unlikely to be significant in the Zn–Al eutectoid alloy because of evolution of fine microstructure by spinodal decomposition. In view of this observation on the sensitivity of the shape of the stress–strain rate curve to the nature of prestrain despite the similar scale of microstructure, the interpretation of Region I of low rate sensitivity in terms of a distinct flow mechanism becomes untenable. The alternative interpretation of Region I in terms of a threshold stress for superplastic flow needs to be considered. In this interpretation, the differences in the stress–strain rate response may arise from variations in threshold stress because of prestrain

TABLE I Grain size and threshold stress data for specimens of varying prestrain

Test temperature (K)	Prestrain history ($\varepsilon = 0.4$)	Grain size[a], d (μm)		Threshold stress, σ_0 (MPa)	$\bar{K}$ (MPa s^m)	m
		Shoulder	Gauge			
448	No prestrain	1.7 ± 0.1	–	2.1	$\bar{K} = 218$	0.40
	Prestrained in Region II ($\dot{\varepsilon} = 1.2 \times 10^{-2}\ s^{-1}$)	1.5 ± 0.1	1.7 ± 0.1	2.0		
	Prestrained in Region I $\dot{\varepsilon} = 1.2 \times 10^{-4}\ s^{-1}$)	1.9 ± 0.2	2.1 ± 0.3	2.3		
473	No prestrain	1.4 ± 0.1	–	0.5	$\bar{K} = 157$	0.40
	Prestrained in Region II ($\dot{\varepsilon} = 1.2 \times 10^{-2}\ s^{-1}$)	1.4 ± 0.1	1.6 ± 0.2	0.4		
	Prestrained in Region I ($\dot{\varepsilon} = 1.2 \times 10^{-4}\ s^{-1}$)	1.5 ± 0.1	1.8 ± 0.2	1.3		
473	No prestrain	2.9 ± 0.3	–	1.1	$\bar{K} = 557$	0.45
	Prestrained in Region II $\dot{\varepsilon} = 6 \times 10^{-3}\ s^{-1}$)	3.4 ± 0.4	3.8 ± 0.7	0.5		
	Prestrained in Region I $\dot{\varepsilon} = 6 \times 10^{-5}\ s^{-1}$)	3.5 ± 0.5	4.3 ± 1.0	1.2		

[a]At 95% confidence level ($d = 1.75\bar{l}$).

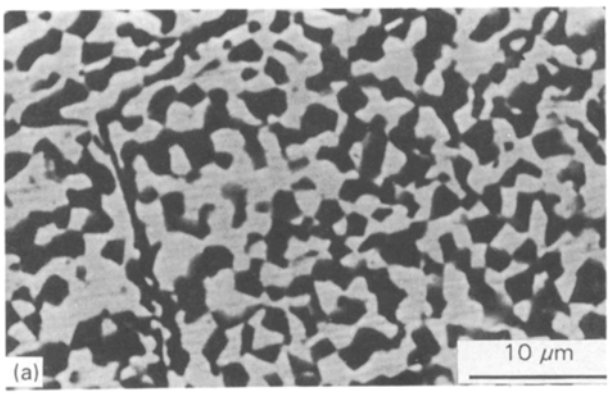

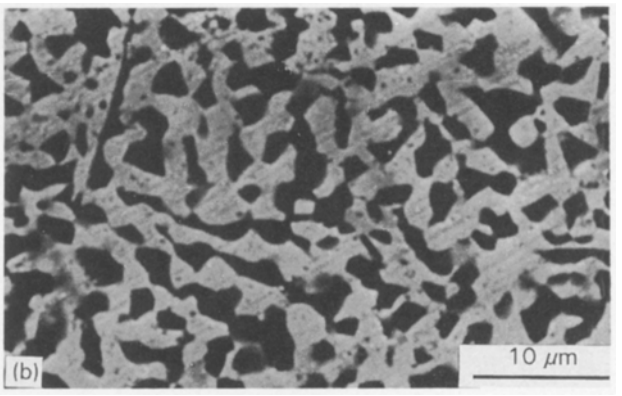

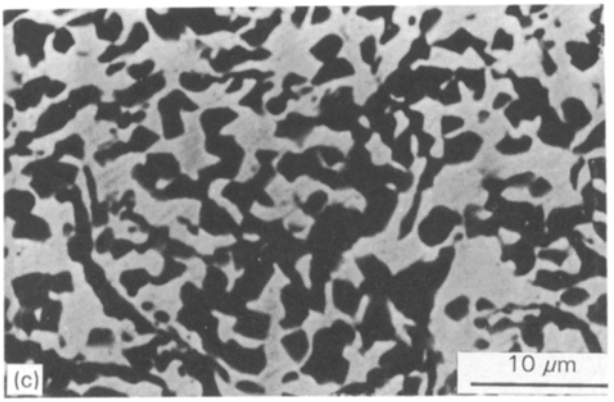

Figure 4 Scanning electron micrographs of specimens (a) without prestrain ($d = 2.9$ μm), (b) prestrained to $\varepsilon = 0.4$ at a strain rate in Region II ($d = 3.4$ μm) (c) prestrained to $\varepsilon = 0.4$ at a strain rate in region I ($d = 3.5$ μm).

history. This aspect is examined by evaluating the threshold stress for superplastic flow in specimens of varying prestrain history. The constitutive equation for superplastic flow in general can be considered as [1]

$$\sigma = \sigma_0 + K\dot{\varepsilon}^m \quad (1)$$

where σ_0 (threshold stress) and K are constants sensitive to temperature and grain size. More explicitly K (T, d) can be expressed as

$$K \propto (e^{mQ/RT})d^{pm} \quad (2)$$

where Q is the activation energy for superplastic flow, R the gas constant and p the grain-size exponent. On the basis of Equation 1, σ_0 for a given grain size and test temperature can be evaluated by extrapolating the double linear plot of σ versus $\dot{\varepsilon}^m$, where m is the rate sensitivity index of superplastic region. While adopting this procedure to assess the threshold stress in specimens of similar grain size at a particular temperature, some variation in the K values was observed. However, the extent of variation in K at a given temperature is not accountable entirely in terms of grain-size differences between various specimens as in Equation 2. In view of this observation, the threshold stress was evaluated from Equation 1 with a mean value of K for each group of specimens tested at a given temperature. From the threshold stress data thus obtained (Table I), variations in threshold stress can be noted between specimens with and without prestrain. Whereas prestrain in Region I results in a higher threshold stress, the opposite trend is seen for the prestrain in Region II. The extent of variation in

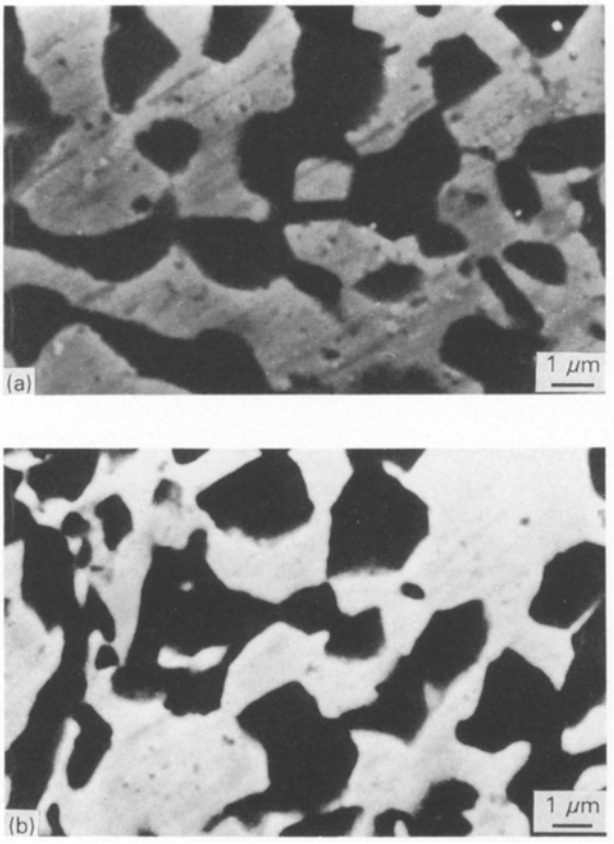

Figure 5 Scanning electron micrographs following a prestrain of $\varepsilon = 0.4$ at a strain rate in (a) Region II ($d = 3.4$ μm) and (b) Region I ($d = 3.5$ μm).

threshold stress differs from one group (specimens tested at one temperature) to the other. It may be noted that comparison of threshold stress data for the two grain sizes at 473 K is, however, not justified because of differences in m between the two cases.

4.2. Microstructural evolution

As already mentioned, the scale of microstructure does not change significantly with the nature of prestrain. Two other microstructural features considered in this investigation are (i) grain-shape factor, and (ii) curvature of grains.

The shape factor, defined as the ratio of maximum dimension of an individual grain to its perpendicular dimension, was estimated for specimens of coarser grain size (~3.4 μm) prestrained in Regions I and II. There is about 40% change in the shape factor of grains as a result of prestrain in Region II, whereas the corresponding change is only 4% for the prestrain in Region I. Thus the grains become elongated in specimens prestrained in Region II, but they remain nearly equiaxed because of prestrain in Region I. An additional feature of interest in this regard is the orientation of grains. The number of linear intercepts per unit length, N_L, can be assessed as a function of orientation (angle Θ) and $N_L(\Theta)$ is plotted to obtain a polar plot. Such a polar plot is observed to be a circle for the microstructures of both the specimens prestrained in Regions I and II. Thus the microstructure in both the cases is random without any alignment of grains.

The average curvature, $\bar{k}$ of phase boundaries in two-dimensional sections of the microstructure is evaluated making use of the relation [14]

$$\bar{k} = 4\{N_A\}_{net}/N_L = 2\{T_A\}_{net}/N_L \quad (3)$$

where $\{T_A\}_{net}$ is the number of net tangents formed by all the arcs in the system, which counts convex tangent as positive and concave tangent as negative, normalized to per unit area of the structure, $\{N_A\}_{net}$ is the algebraic sum of the net subtended angles of each of the closed loops in the structure and N_L is the number of intersections with the grain outline formed by unit length of test line. The calculated values of mean curvature, $\bar{k}$, for differently prestrained specimens are listed in Table II. The curvature of phase boundaries is seen to change significantly with prestrain of Region II, whereas little change occurs in the case of prestrain of Region I. Thus the interphase boundaries tend to be more rounded when prestrained in Region II, compared to the prestrain in Region I. These curvature differences of phase boundaries can also be noted from Fig. 5. Similar observations of rounded grains in superplastic deformation are reported by others [15, 16]. What is striking from the data of Table II is the strong correlation between the changes in curvature of phase boundaries and the threshold stress for superplastic deformation. The more rounded the grains, the lower is the threshold stress.

4.3. Mechanistic interpretation

The above correlation between the changes in threshold stress and the microstructural evolution will now be considered on the basis of the mechanistic origin of threshold stress for superplastic flow. The origin of threshold stress for superplastic flow was discussed in several previous studies [5, 6, 17]. Accordingly, a grain-size and temperature-dependent threshold stress can be explained by the superplastic flow mechanism of grain-boundary sliding (GBS) coupled with a rate-limiting step of grain-boundary migration (GBM). Extensive GBS and GBM are observed during superplastic deformation. While GBM is a fast process at higher stresses, it could be rate-controlling at low stresses if GBM is restricted by solute or particle drag [15]. The migration of the interphase boundaries may also be restricted because of the compositional differences between the phases.

TABLE II Mean curvature and threshold stress data for differently prestrained specimens ($d \simeq 3.4$ μm, $T = 473$ K)

Specimen prestrain history	No prestrain	Prestrained to $\varepsilon = 0.4$ at $\dot{\varepsilon} = 6 \times 10^{-3}\ s^{-1}$ (Region II)	Prestrained $\varepsilon = 0.4$ at $\dot{\varepsilon} = 6 \times 10^{-5}\ s^{-1}$ (Region I)
Mean curvature, $\bar{k}$ (μm^{-1})	0.19	0.24	0.19
(% change)	–	(+26)	(0)
Threshold stress, σ_0 (MPa)	1.1	0.5	1.2
(% change)	–	(−55)	(+9)

The threshold stress can then arise from the drag force on the boundaries.

The driving force for GBM depends on the curvature of the boundaries. The curvature of the rounded grains being larger than flat boundaries, the migration rate of more rounded phase boundaries will be higher. In this mechanism of GBS controlled by GBM, the threshold stress is expected to be low when the migration rate of the boundaries is high. Thus the threshold stress would be lower in specimens prestrained in Region II as compared to those prestrained in Region I because of the observed curvature differences in the microstructures evolved in the two cases of prestrain.

5. Conclusions

1. The stress–strain rate curves of differently prestrained specimens differ in the low strain-rate regime despite the similarity of their grain sizes.

2. Prestraining at a strain rate characteristic of Region I makes Region I more prominent, whereas prestrain in region II tends to eliminate Region I.

3. The threshold stress for superplastic flow decreases significantly with prestrain in Region II, whereas it tends to increase with prestrain in Region I.

4. As a result of prestrain in Region II, the phase boundaries become rounded and their curvature is higher. On the other hand, prestrain in Region I does not alter the curvature of boundaries.

5. The correlation between the changes in threshold stress and curvature of phase boundaries arising from prestrain history is in agreement with the migration-controlled boundary sliding mechanism for the threshold stress.

References

1. W. A. BACKOFEN, F. J. AZZARTO, G. S. MURTY and S. W. ZEHR, in "Ductility" (American Society for Metals, Metals Park, OH, 1968) p. 279.
2. M. L. VAIDYA, K. L. MURTY and J. E. DORN, *Acta Metall.* **21** (1973) 1615.
3. F. A. MOHAMED and T. G. LANGDON, *ibid.* **23** (1975) 117.
4. R. S. MISHRA and G. S. MURTY, *J. Mater. Sci.* **23** (1988) 593.
5. F. A. MOHAMED, *ibid.* **18** (1983) 582.
6. P. K. CHAUDHARY, V. SIVARAMAKRISHNAN and F. A. MOHAMED, *Metall. Trans.* **19A** (1988) 2741.
7. F. A. MOHAMED, S. A. SHEI and T. G. LANGDON, *Acta Metall.* **23** (1975) 1443.
8. F. A.MOHAMED and T. G. LANGDON, *Philos. Mag.* **32** (1975) 697.
9. G. S. MURTY and M. J. KOCZAK, *Mater. Sci. Eng.* **96** (1987) 117
10. G. S. MURTY and M. J. KOCZAK, "Superplasticity and Superplastic Forming", edited by C. H. Hamilton and N. E. Paton (TMS–AIME, Warrendale, PA, 1988) p. 27.
11. G. S. MURTY, in "Superplasticity in Advanced Materials", edited by S. Hori, M. Tokizane and N. Furushiro (The Japan Society for Research on Superplasticity, 1991) p. 45.
12. *Idem, Scripta Metall.* **20** (1986) 533.
13. W. A. BACKOFEN, I. R. TURNER and D. H. AVERY, *Trans. ASM* **57** (1964) 980.
14. R. T. DeHOFF, *Trans. Metall. Soc. AIME* **239** (1967) 617.
15. R. C. GIFKINS, in "Superplastic Forming of Structural Alloys", edited by N. E. Paton and C. H. Hamilton (TMS–AIME, Warrendale, PA, 1982) p. 3.
16. D. M. R. TAPLIN, G. L. DUNLOP and T. G. LANGDON, *Ann. Rev. Mater. Sci.* **9** (1979) 151.
17. G. S. MURTY and M. J. KOCZAK, *J. Mater. Sci.* **24** (1989) 510.

Received 9 November 1992
and accepted 7 May 1993